Determining the Faulted Phase

David Costello and Karl Zimmerman
Schweitzer Engineering Laboratories, Inc.

Revised edition released December 2015

Previously presented at the
63rd Annual Conference for Protective Relay Engineers, March 2010

Previous revised editions released July 2010, March 2010, and October 2009

Originally presented at the
36th Annual Western Protective Relay Conference, October 2009

Determining the Faulted Phase

David Costello and Karl Zimmerman, *Schweitzer Engineering Laboratories, Inc.*

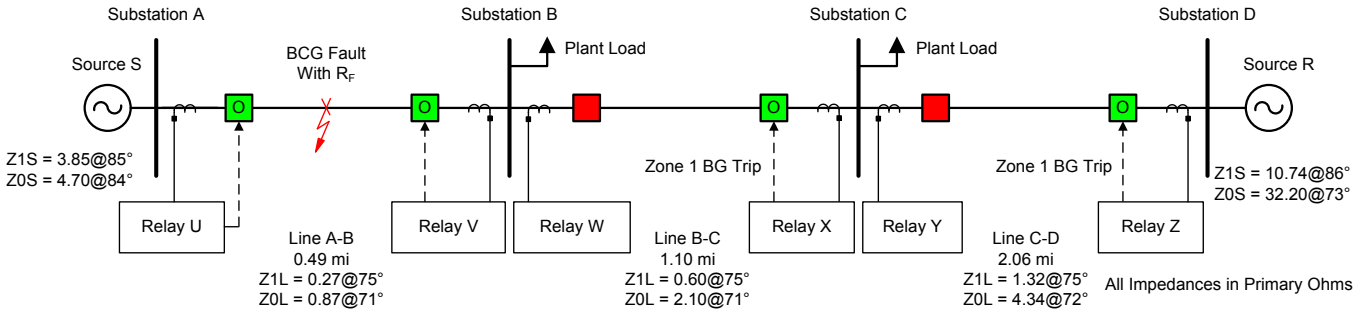

Fig. 1. Case Study Number 1 One-Line Diagram

***Abstract*—In August 1999, a lightning strike caused a misoperation of a relay installed in the late 1980s. The relay misoperation caused a two-minute outage at a petrochemical plant and led to an exhaustive root-cause analysis. The misoperation can be attributed to incorrect fault type selection in a distance element-based, 1980s-era relay.**

Two separate events in different locations, one in December 2007 and another in March 2009, highlight additional incorrect operations that occurred due to the same problem and root cause. The recent events remind us that this topic is still important and should be reviewed.

This paper shares details about three challenging case studies and their root causes. Methodical root-cause analysis techniques are used, including mathematical simulation and testing of old and newer relay designs.

This paper contrasts distance and fault identification algorithms, demonstrates methodical analysis techniques, and proposes solutions. Fault type selection logic is discussed, and the evolution and improvement of faulted phase selection logic over several decades is demonstrated.

A newer relay design, available since 1993, is proven to have improved performance, namely better security, for these challenging cases.

I. Nomenclature

AB, BC, CA, AG, BG, and CG indicate fault types. Additionally, these refer to impedance elements, or loops, within a relay.

Apparent impedance measured by an element may be plotted on an R-X impedance diagram. Additionally, it may be expressed as a number or torque-like product (or more simply, torque). Lower torque is analogous to apparent impedance plotting further from the origin of the R-X diagram. Higher torque is analogous to apparent impedance nearer to the origin.

ABG, BCG, and CAG indicate double line-to-ground fault types.

R_F indicates fault resistance.

Rag, Rbg, Rcg, Rab, Rbc, and Rca indicate fault resistance estimates for the designated fault types.

II. Introduction

In August 1999, a thunderstorm and lightning strike caused a BCG fault with ground fault resistance (R_F) on a 138 kV transmission system. This is Case Study Number 1. Refer to Fig. 1 for the one-line diagram. The fault occurred on Line A-B.

All of the relays shown in Fig. 1 are of the same make and model, a 1980s-era microprocessor-based relay. The two relays closest to the fault, Relays U and V, operated correctly and as expected to de-energize and quarantine the faulted portion of the power system.

A single plant load is served from Substations B and C. For this fault, the plant was expected to have temporarily lost one source, Source S, but remain energized and in operation by service from Source R. However, Relays X and Z operated unexpectedly during the fault. Each of these relays identified the fault as Zone 1 BG and operated with no intentional time delay. Zone 1 would normally indicate that a fault was not located beyond the remote line terminal.

This resulted in the de-energization of Substations B and C and loss of source power to the entire plant. The outage lasted for two minutes. Reduced plant production rates were endured because startup procedures took several days to complete [1].

In December 2007, a CAG fault with R_F occurred on a transmission line. This is Case Study Number 2. Refer to the one-line diagram in Section VI. The fault was located in the line section—just at or beyond the Zone 1 reach. The relays at each end of the line tripped to clear the fault, so the utility determined this operation to be "correct." However, upon further inspection, it can be seen that one relay determined the fault type to be Zone 1 CG and possibly overreached. While it is desirable to trip high speed for an in-section fault, from a manufacturer's perspective, this event would be classified as an incorrect operation. The relay involved in Case Study Number 2 is the same model as those in Case Study Number 1.

In March 2009, an ABG fault with R_F occurred on a 138 kV transmission line. This is Case Study Number 3. Refer to the one-line diagram in Section VII. The relays closest to the fault correctly tripped. One line section away, a relay incorrectly identified the fault type to be a Zone 1 AG and overreached. This caused a momentary outage of a distribution substation until automatic reclosing restored service. The relay involved in Case Study Number 3 is not the same model as those in Case Study Number 1; however, they share fault type selection and distance element algorithm design.

In all cases, an investigation of the relay misoperations began immediately. Engineers from the local utility and the relay manufacturer cooperated and determined the root cause of the relay overreach. These engineers identified short- and long-term solutions and began implementing both solutions immediately. The short-term solutions involved performing system fault studies and changing settings in each 1980s-era relay. Long-term solutions involved upgrading to newer relay technology (available since 1993) that offered significant performance improvements.

III. Distance Element Evolution

Self-polarized mho elements implemented in traditional (typically, electromechanical) relays have a reach setting Zr, which represents the diameter of a circular characteristic passing through the origin on the R-X plane. These elements offer no expansion for R_F coverage and are not reliable for zero-voltage faults.

Traditional elements with cross-polarization expand toward the source impedance during faults. This improves R_F coverage. However, these elements are also unreliable during zero-voltage, three-phase faults.

Positive-sequence memory polarization implemented in traditional relays provides reliable operation for zero-voltage faults until the polarizing memory expires (typically 2 to 3 cycles). These elements also expand in proportion to the source impedance to provide the greatest R_F coverage. See Fig. 2.

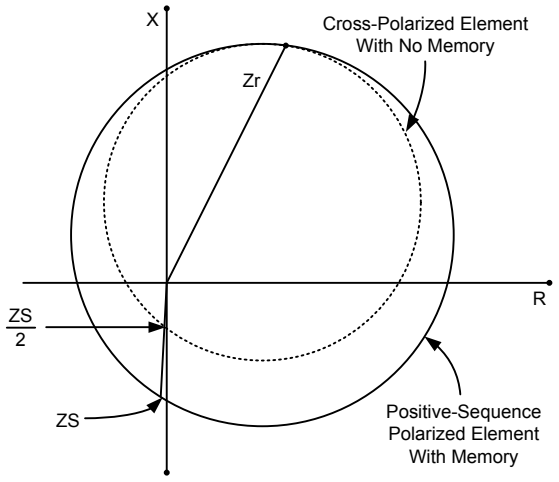

Fig. 2. Phase-to-Phase Element Response for a Forward Phase-to-Phase Fault

While expanded and dynamic mho elements offer better R_F sensitivity, they are also more likely to operate for unintended fault types as compared to self-polarized mho elements.

To illustrate how uninvolved phase and ground distance elements pick up for an AG fault on a radial system, consider Fig. 3. Fault location and fault impedance are varied. For each fault simulation, the torques for six Zone 3 elements (AB, BC, CA, AG, BG, and CG) are calculated. The Zone 3 reach is set to 300 percent of the line impedance.

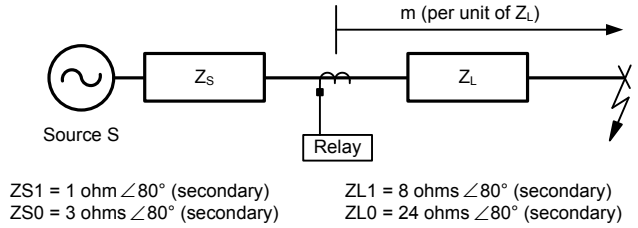

Fig. 3. Example One-Line Diagram Illustrating Distance Element Response for an AG Fault

The first step is to place an AG fault at the local bus (m = 0), vary the R_F from 0 to 4 ohms secondary, and plot the results. Fig. 4 shows the results of this exercise.

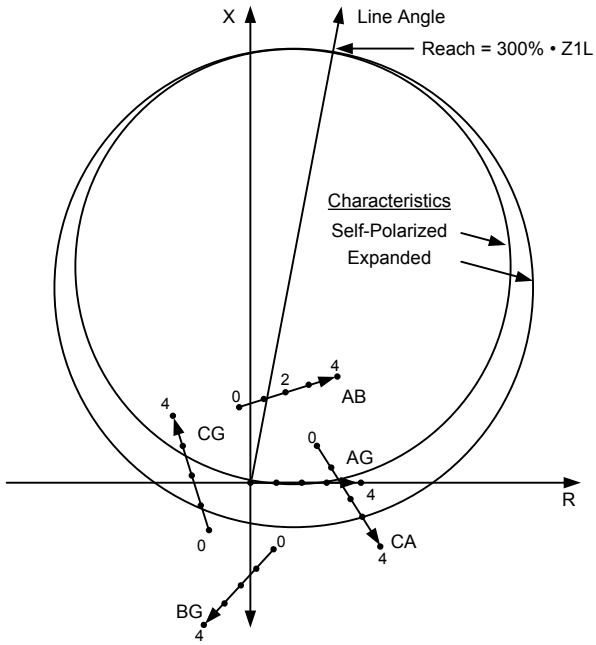

Fig. 4. Apparent Impedances Seen by Varying R_F for a Close-In AG Fault

Several observations can be made from Fig. 4. Multiple distance elements detect the AG fault when $R_F = 0$. Also, the number of elements that detect the fault varies with R_F.

The second step is to vary the distance to the fault from m = 0 to m = 1 (100 percent of the protected line). In this step, R_F is not considered. Fig. 5 shows the results of this exercise.

Several observations can be made from Fig. 5. All distance elements involved with A-phase pick up for AG faults near the bus. As the fault location is moved away from the local bus, the torque produced by these elements decreases. For a fault at m = 1, only the AG element detects the fault.

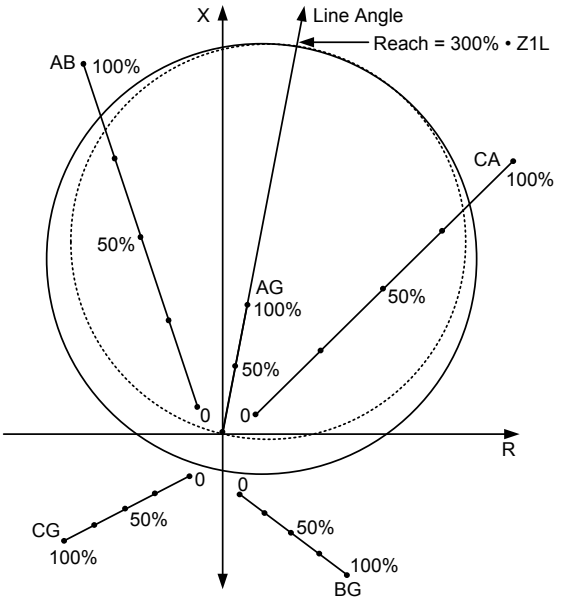

Fig. 5. Apparent Impedances Seen by Varying Fault Location (Without R_F)

Fig. 6 superimposes Fig. 4 and Fig. 5. This illustrates a portion of the fault condition spectrum that causes apparent impedance for an AG fault to be seen by multiple mho elements.

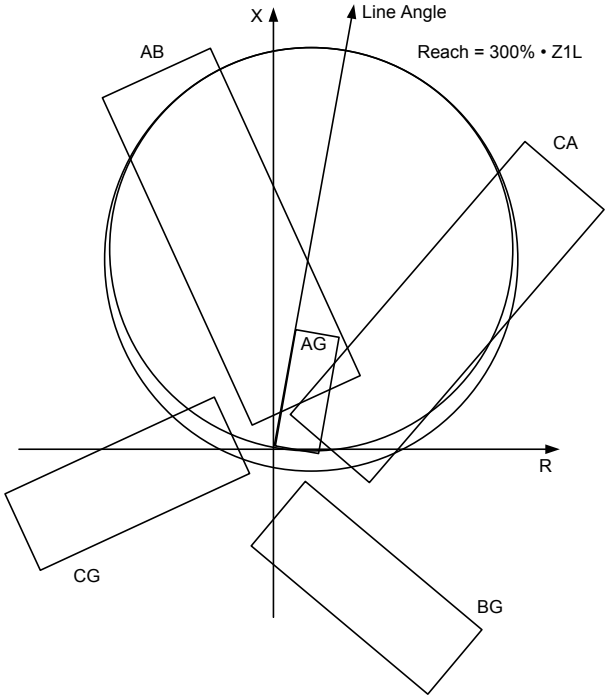

Fig. 6. Fig. 4 and Fig. 5 Superimposed

IV. Determining the Faulted Phase

A variety of methods have been used to correctly identify the fault type and enable appropriate elements for operation.

In single-pole applications, the correct faulted phases must be identified and opened (phase-to-phase elements must be blocked for single line-to-ground faults). In all applications, it is important that distance elements not overreach. For double line-to-ground faults (e.g., BCG) with R_F, the ground element associated with the leading phase (BG) tends to overreach.

Real power systems offer no shortage of challenging variables for relay algorithms: line length, source strength, power flow, fault location, fault type, R_F, and relay settings. Indeed, improving the performance of fault type selection algorithms, especially with regard to preventing the overreach of Zone 1 phase-to-ground elements for phase-to-phase faults with R_F, is a research priority and the focus of technical literature for many individuals and manufacturers that continues to this day [2].

In general, fault-selection logic is only present to prevent an incorrect operation. That is, fault-selection logic does not produce a trip decision; it only supervises the operation of certain elements (e.g., a phase-to-phase fault selection prevents a phase-to-ground distance element from overreaching for a phase-to-phase-to-ground fault).

A. Relay Fault Type Selection—1980s Design

The 1980s-era microprocessor relay utilized throughout the system in Fig. 1 uses positive-sequence memory voltage polarized mho distance elements for three-zone phase and ground distance protection [3]. The microprocessor implementation allowed for longer memory than traditional relays (about 10 cycles).

This relay introduced a new method (at the time) for faulted phase identification. It was not possible to evaluate the torque for all six distance elements (AB, BC, CA, AG, BG, and CG) in all three zones every quarter-cycle processing interval in an eight-bit microcontroller. Instead, the computer calculates the six Zone 3 torque products and tests their signs.

Each element's torque is the result of (1), substituting the appropriate voltages and currents from Table I.

$$T = \mathrm{Re}\left[\left(Z_r \bullet I - V\right) \bullet VP^*\right] \tag{1}$$

Table I shows the voltage and current combinations used to calculate the torque of each distance element.

TABLE I
VOLTAGES AND CURRENTS USED IN (1)

Element	Voltage (V)	Current (I)	Polarization (VP)	Torque (T)
AG	VA	IA + K • IR	VAlm	Tag
BG	VB	IB + K • IR	VBlm	Tbg
CG	VC	IC + K • IR	VClm	Tcg
AB	VA – VB	IA – IB	–j • VClm	Tab
BC	VB – VC	IB – IC	–j • VAlm	Tbc
CA	VC – VA	IC – IA	–j • VBlm	Tca

m: denotes memory voltage

K = 1/3 (Zo/ZL – 1) … residual current compensation factor

Positive products indicate impedances inside the expanded mho circle characteristics. A larger number indicates stronger torque or a fault nearer the origin [4].

With respect to an overreaching element such as Zone 3, comparing torque was a useful and computationally efficient fault type discriminant. In other words, every quarter cycle, the Zone 3 mho elements update and present their operate/restraint state and torque value to a fault identification (lookup) table. Essentially, with a few qualifiers, the loop (AB, BC, CA, AG, BG, and CG) that has the highest positive torque product is declared the fault type [5]. Once the fault type is selected, corresponding impedance elements are allowed to operate.

Early technical literature identifies a weakness with selectivity in this scheme. Zone 1 must not operate for a fault beyond the remote bus. A double line-to-ground fault with R_F tends to cause the ground element associated with the leading phase to overreach for certain values of R_F. The relay scheme must, therefore, correctly block the ground distance elements for these faults.

The success of determining fault type by comparing Zone 3 element torques is dependent on the reach setting and R_F. To illustrate this, the system in Fig. 1 was modeled. A BCG fault was placed near Substation A. Torque products for the BC and BG Zone 3 elements in Relay Z were calculated for several values of R_F and Zone 3 reach using the Mathcad® worksheet shown in the appendix [6]. Fault impedance was varied from 0 to 4 ohms. Several values of Zone 3 reach were evaluated: 155 percent, 310 percent, and 620 percent of the protected Line C-D impedance. The results of this exercise are shown in Fig. 7.

Several interesting observations can be made from Fig. 7. With a Zone 3 reach setting at 155 percent of Line C-D, the relay incorrectly identifies the fault type as BG for R_F up to 3 ohms. Increasing the Zone 3 reach setting to 310 percent allows for correct BC fault type selection near 1 ohm R_F and for R_F values of about 1.5 ohms and above. However, for R_F values near 1 ohm, the relay incorrectly identifies the fault type as BG. Increasing the Zone 3 reach setting to 620 percent ensures that the relay makes the correct BC fault type selection for all values of R_F.

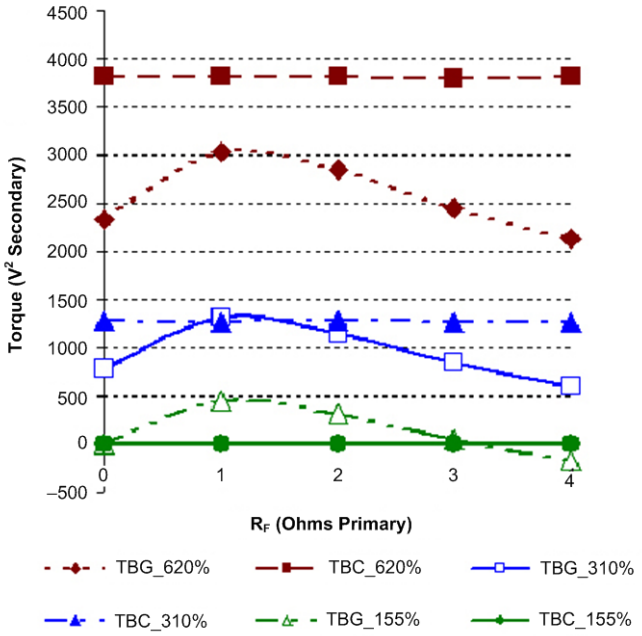

Fig. 7. BG and BC Torque Values for Different R_F and Zone 3 Reach

The conclusion drawn from Fig. 7 is that larger Zone 3 reach settings provide more reliable fault type selection when using torque comparison.

Several applications may complicate the user's ability to implement the Zone 3 reach in this manner. If the relay is used in a short-line (or a series of short lines) application as in Fig. 1, reach settings may be set small. Also, if Zone 3 is relied upon to provide backup protection for complete failures at the remote station, such as a dc battery failure, it will be set to trip and must coordinate with remote relays. Short-line applications or those with Zone 3 used as backup, therefore, conspire against the recommended practice of setting Zone 3 larger to ensure proper fault type selection.

With this relay, the engineer must model the power system, perform fault studies, and examine fault type selection based on Zone 3 torques to ensure the applied settings are secure.

B. Fault Type Selection—Today

In 1993, a distance relay design introduced several innovations that are still state-of-the-art at the writing of this paper (2009) [7]. These innovations include:

- A computationally efficient numerical method of characterizing distance elements onto a single point on a number line. This allows all six impedance loops (AB, BC, CA, AG, BG, and CG) for multiple zones (e.g., four zones of distance element protection) to be calculated, measured, and compared every processing interval (e.g., every 1/8 cycle) [8].
- Positive-sequence memory polarization that allows distance elements to retain directional security for close-in, low- (or zero-) voltage faults for over 1 second. This is particularly important for the application of distance elements on short lines.

- Fault identification selection (FIDS) logic that uses measured negative- (IA2) and zero-sequence (IA0) currents. This method is *not* settings-dependent and addresses two major concerns: 1) that ground distance elements do not overreach for line-to-line-to-ground (LLG) faults, and 2) that phase distance elements do not operate for close-in, line-to-ground (LG) faults [9].

The FIDS logic in the modern design compares the angle between IA0 and IA2 (referenced to A-phase). Fig. 8 shows that IA0 and IA2 are in phase for AG and BCG faults without R_F.

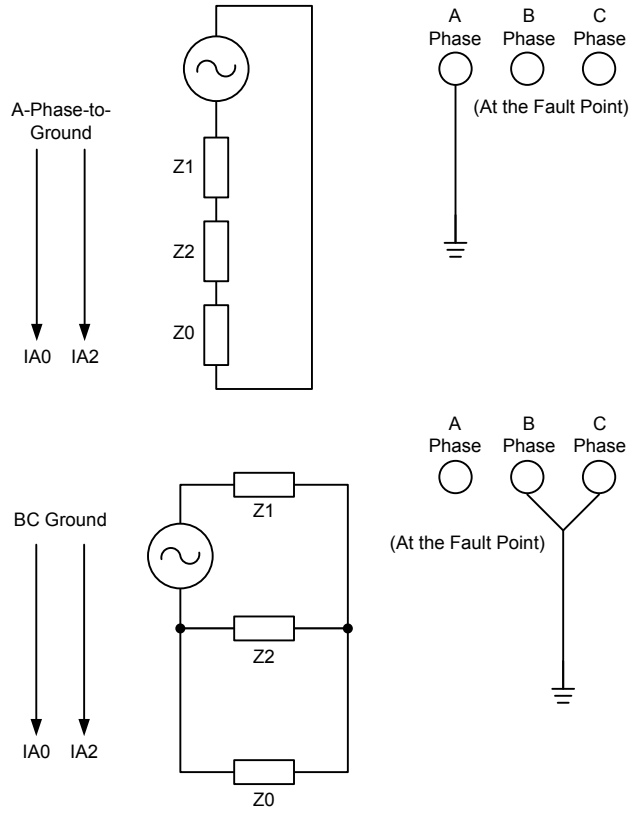

Fig. 8. IA0 and IA2 Relationship for AG and BCG Faults (Without R_F)

Fig. 9 shows the IA0 and IA2 relationships for AG, BG, and CG faults. Note that IA2 lags IA0 for a BG fault, but IA2 leads IA0 for CG faults. Thus by creating "sectors," we can use these relationships to determine fault type.

As we add R_F, these angles increase. For a system with the source and line impedances shown in the legend in Fig. 10, as R_F increases, IA2 lags IA0 by an increasing angle. When the angle is more than 30 degrees from its expected value, we can compare the phase and ground R_F estimates and select the fault type with the minimum absolute value of resistance. For example, if we refer to Fig. 10, a comparison of |Rag| against |Rbc| would reveal that |Rag| is much larger than |Rbc|. Therefore, the logic selects BC (over AG) as the fault type.

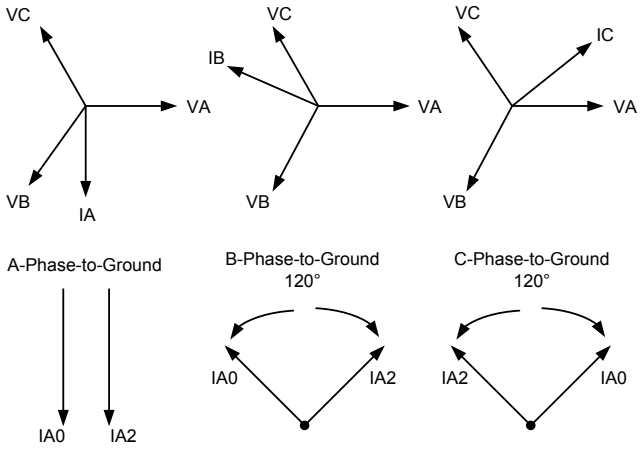

Fig. 9. IA0 and IA2 Relationship for AG, BG, and CG Faults

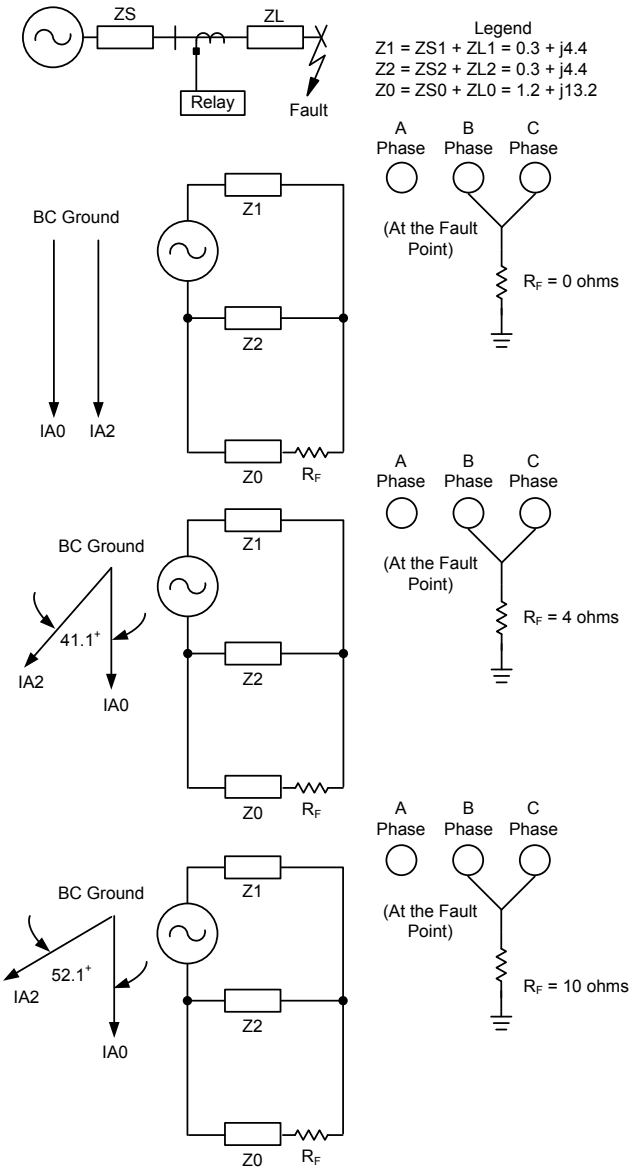

Fig. 10. Effects of Increasing R_F for a BCG Fault

Reference [7] derives the fault resistance test used by the modern relay for an AG fault using single-ended relay data. Refer to the one-line diagram in Fig. 1. For an AG fault on the system, the A-phase-to-ground voltage at Substation D is given by (2).

$$V_A = m \bullet ZlL \bullet \left(I_{AD} + k_0 \bullet I_{RD}\right) + Rag \bullet I_F \quad (2)$$

where:

V_A = A-phase voltage measured at Substation D.

m = per-unit distance to the fault from Substation D.

ZIL = positive-sequence line impedance.

Rag = A-phase-to-ground fault resistance.

I_F = total current flowing through R_F.

I_{AD} = A-phase current measured at Substation D.

I_{RD} = residual current measured at Substation D ($3I_{0D}$).

The goal is to extract an R_F estimate from (2). In the discussion above, this estimate is referred to as Rag. To eliminate the unknown *m* term, multiply each side of the equation by the complex conjugate of the line-drop voltage term m • Z1L • (I_{AD} + k_0 • I_{RD}), and save the imaginary components. Let I_F = 3/2 (I_{2D} + I_{0D}), where I_{2D} and I_{0D} are the Substation D negative- and zero-sequence currents, respectively. This approximation takes into account only Substation D currents available to Relay Z, is independent of balanced load due to the exclusion of the positive-sequence current, and ensures that the relay measures the true R_F on a radial system. Solving for Rag, we derive (3).

$$Rag = \frac{Im\left[V_A \bullet \left(ZlL \bullet \left(I_{AD} + k_0 \bullet I_{RD}\right)\right)^*\right]}{Im\left[1.5 \bullet \left(I_{2D} + I_{0D}\right) \bullet \left(ZlL \bullet \left(I_{AD} + k_0 \bullet I_{RD}\right)\right)^*\right]} \quad (3)$$

Infeed from Substation A causes the R_F estimate to increase, because the calculation does not include any measurement of current from the remote terminal. For example, if the impedances on either side of the fault are equal, Rag is twice the actual fault resistance.

Similar R_F estimates are calculated for the other fault types. In calculating Rbg, Rcg, Rab, Rbc, and Rca, equations similar to (3) are used, substituting different fault voltages and currents that are appropriate for those fault types.

The fault type selection process of the modern relay is summarized in Table II. Fig. 11 and Fig. 12 are graphical representations of the phase angle sectors identified and used by the modern fault type selection algorithm.

The angle of IA2 is compared to the angle of IA0. In Fig. 11, if IA2 is in phase with IA0 (±30 degrees), then the fault type is either AG or BC. In this sector (yellow), the relay selects AG or BC based on which element has the lowest calculated reach. If IA2 lags IA0 by 120 degrees (±30 degrees), then the fault type is either BG or CA. In this sector (red), the relay selects BG or CA based on which element has the lowest calculated reach. If IA2 leads IA0 by 120 degrees (±30 degrees), then the fault type is either CG or AB. In this sector (green), the relay selects CG or AB based on which element has the lowest calculated reach. By virtue of its design, this logic selects the noninvolved phase loop for phase-to-phase-to-ground faults with limited R_F.

Table II summarizes the modern design FIDS logic.

TABLE II
FIDS LOGIC IN MODERN DESIGN

Angle Between IA2 and IA0	Fault Type Permission
IA2 is ±30 degrees of IA0	Permit AG or BC. Select A-phase or B-C-phase based on the lowest mho element calculated reach.
IA2 lags IA0 by 90 to 150 degrees	Permit BG or CA. Select B-phase or C-A-phase based on the lowest mho element calculated reach.
IA2 leads IA0 by 90 to 150 degrees	Permit CG or AB. Select C-phase or A-B-phase based on the lowest mho element calculated reach.
IA2 leads or lags IA0 by 30 to 60 degrees	Select the phase-to-phase mho element with the lowest calculated reach. Compare |Rag| with the |R_F| of that element. If |Rag| is lower, the fault involves A-phase. If not, select the phase-to-phase element.
IA2 lags IA0 by 60 to 90 degrees or 150 to 180 degrees	Select the phase-to-phase mho element with the lowest calculated reach. Compare |Rbg| with the |R_F| of that element. If |Rbg| is lower, the fault involves B-phase. If not, select the phase-to-phase element.
IA2 leads IA0 by 60 to 90 degrees or 150 to 180 degrees	Select the phase-to-phase mho element with the lowest calculated reach. Compare |Rcg| with the |R_F| of that element. If |Rcg| is lower, the fault involves C-phase. If not, select the phase-to-phase element.

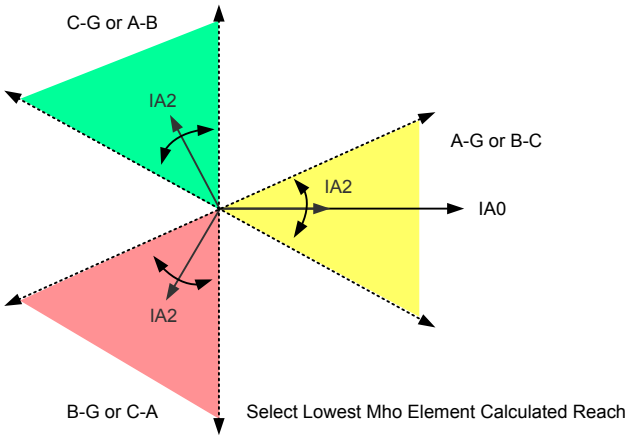

Fig. 11. Graphical Representation of Table II Showing Primary 60-Degree Sectors

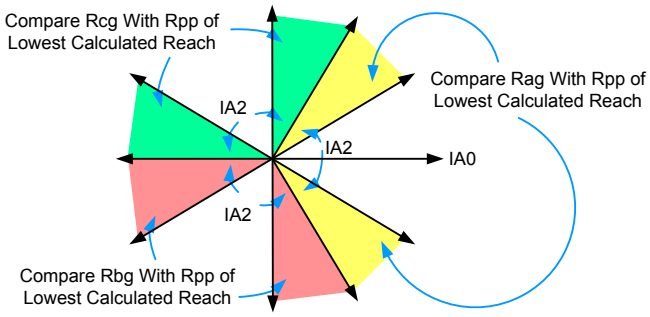

Fig. 12. Graphical Representation of Table II Showing Secondary 60-Degree Sectors

Increasing R_F causes the angle of IA2 to fall outside the primary phase angle sectors shown in Fig. 11. See Fig. 12. When IA2 lies in one of these secondary phase angle sectors, the modern relay first selects the phase-to-phase mho element with the lowest calculated reach. If IA2 lies in the yellow sectors, the modern relay compares the absolute values of the resistance calculations for Rag and the phase-to-phase element with the lowest calculated reach. If |Rag| is lower, the relay selects an AG fault type; otherwise, the phase-to-phase element is selected. If IA2 lies in the red sectors, the relay compares the absolute values of the resistance calculations for Rbg and the phase-to-phase element with the lowest calculated reach. If |Rbg| is lower, the relay selects a BG fault type; otherwise, the phase-to-phase element is selected. If IA2 lies in the green sectors, the relay compares the absolute values of the resistance calculations for Rcg and the phase-to-phase element with the lowest calculated reach. If |Rcg| is lower, the relay selects a CG fault type; otherwise, the phase-to-phase element is selected.

C. How Would the Modern Relay Select the Fault Type for the Case Study Number 1 (August 1999) Event?

Fig. 13 shows the relationship between IA0 and IA2 from the actual Relay Z fault data. IA2 lags IA0 by 49 degrees. This phase angle relationship is outside the primary sectors in Fig. 11. Therefore, the relay selects the phase-to-phase element with the lowest calculated reach, Mbc. See Table III. Because IA2 is within ±60 degrees of IA0 (in the yellow secondary sectors in Fig. 12), the relay compares the absolute values of the resistance estimates for Rag and the selected phase-to-phase element (Rbc). Because Rbc is the lowest (Rag is actually ignored in this case, because it is a negative value), the FIDS logic selects BC. Recall that the actual fault type is BCG, and a BC fault type declaration is desired. Recall also that the 1980s design incorrectly declared a BG fault type and overreached.

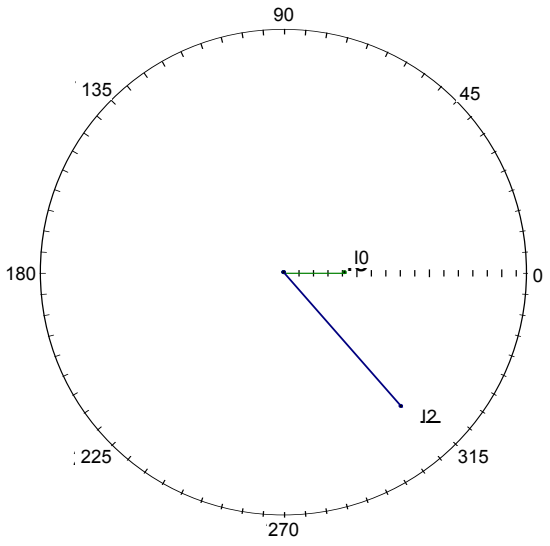

Fig. 13. Event Data From Relay Z During the Fault at Cycle 7

TABLE III
MODERN DESIGN MHO REACH AND R_F CALCULATIONS FROM SUBSTATION D DATA DURING THE FAULT AT CYCLE 7

Fault Identification Angle: ang (Ia0) – ang (Ia2) = 48.88 degrees			
Mho Reach		**Fault Resistance**	
Mag = –12	Mab = 4.44	Rag = –1.46	Rab = 14.25
Mbg = 0.2	**Mbc = 0.44**	Rbg = 1.18	**Rbc = 0.28**
Mcg = 1.44	Mca = 7.5	Rcg = 0.19	Rca = –11.9

V. FINDING ROOT CAUSE—CASE STUDY NUMBER 1

A. Analysis of the Fault

For Case Study Number 1, the first step in determining root cause is to ask what was expected to happen. Refer to Fig. 1 for the one-line diagram. Refer to Fig. 14 for the fault data from Relay Z. For a BCG fault near Bus A, we expected the nearest terminals (breakers for Relays U and V) to open and experience no other operations.

What actually happened? Operation logs from the utility and inspection of the event reports show that the two terminals closest to the fault did in fact operate, but in addition, two relays overreached (Relays X and Z) and were tripped by Zone 1 BG elements.

We analyzed the event data from the relays that overreached using worksheets similar to the appendix [6]. In both relays, we observed that the Tbg torque product produces the highest positive value. Thus the relays select BG as the fault type. This confirms that the relays operated as designed and set (albeit with an undesired outcome) for this out-of-section fault.

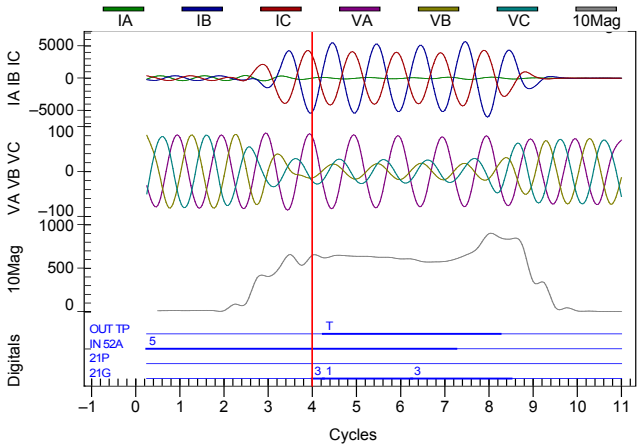

Fig. 14. Event Data From Relay Z Shows BCG Fault and Zone 1 BG Overreach

B. Considerations for Improved Settings in the 1980s Design

Using this same worksheet, we wanted to show some immediate steps that could be taken by the utility to prevent this and other occurrences. See Fig. 15. For example, we show that reducing the Zone 1 reach from the as-set value of 75 percent to 53 percent of the line impedance would have prevented operation (Tbg for Zone 1 becomes negative). We also show that increasing Zone 3 to about 500 percent of the line impedance would have caused the fault-selection logic to perform correctly (Tbc would produce the highest positive value), and again, prevent this operation.

Mho Distance Calculations:

$Re(Tag) = -4.708 \cdot 10^3$ $Re(Tbg) = -1.318$ $Re(Tcg) = -1.407 \cdot 10^3$

$Re(Tab) = -4.555 \cdot 10^3$ $Re(Tbc) = -802.475$ $Re(Tca) = -5.236 \cdot 10^3$

$r \equiv 0.53$

Mho Distance Calculations:

$Re(Tag) = -5.115 \cdot 10^3$ $Re(Tbg) = 2.192 \cdot 10^3$ $Re(Tcg) = -210.06$

$Re(Tab) = -3.126 \cdot 10^3$ $Re(Tbc) = 2.273 \cdot 10^3$ $Re(Tca) = -4.573 \cdot 10^3$

$r \equiv 5.00$

Fig. 15. Short-Term Settings Solutions Where *r* Is the Reach Setting

Extending Zone 3 reach settings is an option that the utility would need to evaluate. For example, if Zone 3 is used as a remote backup (as it was in this case study) for remote breaker failure or station battery failure, extending Zone 3 reach may not be practical.

In short lines (where Z1L is less than 0.5 ohms secondary), Zone 1 reach must often be reduced or should not be used at all for a myriad of reasons. These difficulties include:

- Voltages and currents at the relay for close-in and remote bus faults appear nearly identical on short lines.
- CVT (capacitive voltage transformer) transients are exacerbated by SIRs (source impedance ratios) greater than four.
- Low voltages at the relay (less than 5 V secondary) for three-phase faults require additional directional element security.
- Directional elements must be sensitive enough to see low-voltage faults but not operate for system unbalances.
- PT (potential transformer) accuracy errors increase greatly at low voltages (less than 5 V secondary).
- Fixed relay accuracy errors (as well as modeling errors) play a larger factor in short-reach applications.

Careful system analysis must determine if Zone 1 can be applied on a short line, and if so, at what reduced reach and possible time delay. In some applications, Zone 1 may have to be disabled altogether.

Today, short-line applications often afford inexpensive and reliable communications options (e.g., radio, fiber) for dual primary communications-assisted tripping schemes or line current differential systems to provide instantaneous tripping for faults on the entire line without requiring Zone 1. Compared to their counterparts in the 1980s, today's engineers have better tools available to solve problems. Even still, this discussion highlights the effort required by the user in determining secure settings.

However, as Fig. 15 shows, the setting for Zone 1 reach must also take into account the fault-selection algorithm of the 1980s design, coupled with the Zone 3 setting used and variable system parameters, such as source impedances, fault location, and R_F. To evaluate the relay performance with example settings, we can use Mathcad or Microsoft® Excel® tools and power system fault simulation software, such as ASPEN OneLiner® [6].

C. Simulations Using ASPEN OneLiner

How might an engineer have discovered the potential for a fault-selection problem on this system with these settings?

We modeled the one-line diagram and the electrical system shown in Fig. 1 using ASPEN OneLiner (see Fig. 16). A BCG fault with 0.92-ohm fault resistance was simulated on Line A-B at 98 percent of the line (toward Substation A, from Substation B). ASPEN OneLiner simulates the electrical system, calculates the fault voltage and currents, and presents the relay response. The software includes a model of the 1980s relay.

The simple apparent impedances shown in Fig. 16 do not plot within the mho circles. However, ASPEN OneLiner emulates the torque equations shown in Table I. The results of these equations are shown as the relay response in the rectangles. Notice the "C to B Ground Relay" BG element shows "Zone 1 Tripped." This corresponds to Relay X on the one-line diagram in Fig. 1 and matches the observed operation in the field.

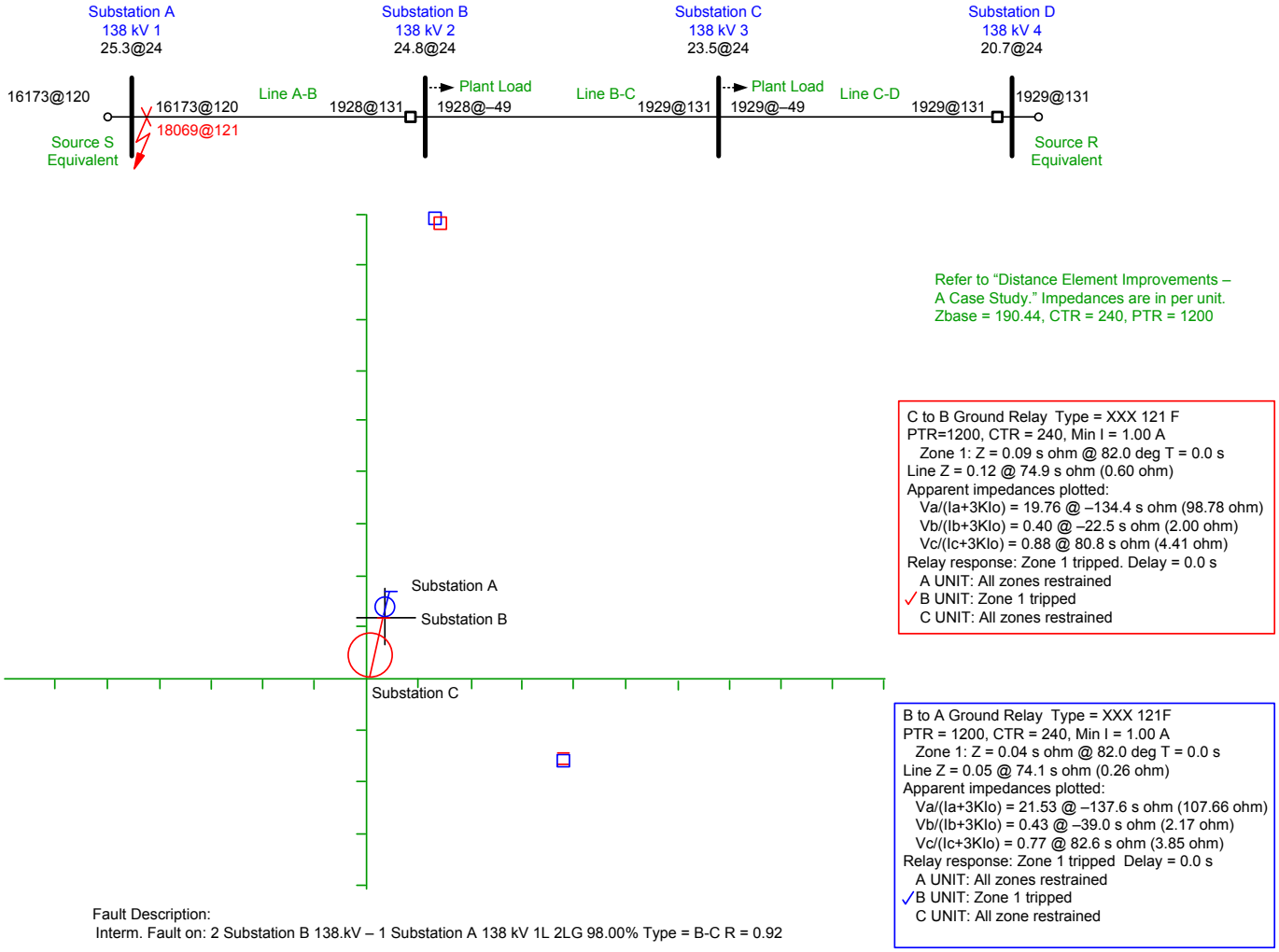

Fig. 16. Case Study Number 1—Fault Near A, Relay Z Response ASPEN OneLiner Model

Without prior knowledge of fault location and R_F, we would have to run a series of sliding faults at increments of the line with fault resistance estimates of varying amounts and observe the behavior of the phase-to-ground elements for phase-to-phase faults. ASPEN OneLiner does not simulate the actual 1980s fault-selection process, which is a so-called "zone switching" or "fault throwing switch" algorithm. However, overreach in the simulation shown in Fig. 16 validates the claim that the ground distance element associated with the leading phase of a phase-to-phase-to-ground fault may overreach. This observation would have alerted an engineer to investigate the relay response and settings solutions.

D. Replay of Original Fault Data Using COMTRADE Into the 1980s-Era Microprocessor Relay

To further validate our Mathcad model and theory, the event report data recorded by Relay Z during the 1999 BCG fault were converted to COMTRADE files and replayed into a relay in the lab. The relay was the same model, the 1980s-era microprocessor relay described earlier.

In the first test, Zone 1 was set to 75 percent, and Zone 3 was set to 155 percent of the Line C-D impedance. These settings match those installed in Relay Z during the fault. The relay Zone 3 BG element sees the fault and determines the fault to be a BG fault type. Once enabled incorrectly by the fault-selection logic, the Zone 1 BG element operates and overreaches. The results of this test are shown in Fig. 17. This test simply confirmed the operation of the relay in the field and our ability to duplicate its operation in the lab.

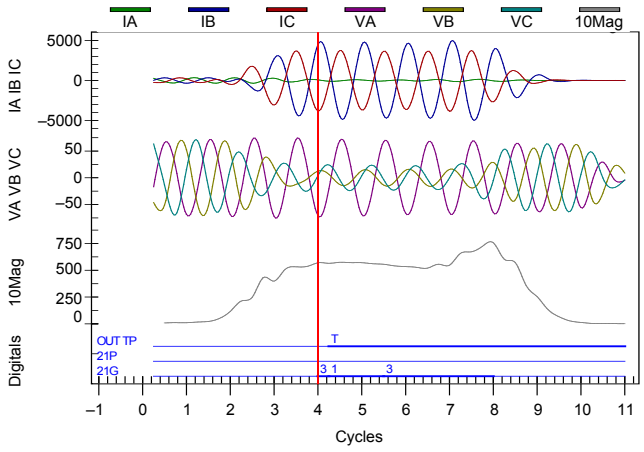

Fig. 17. Zone 1 at 75 Percent, Zone 3 at 155 Percent as Set—Replay Shows Trip

In the second test, Zone 1 reach was left at 75 percent, and the Zone 3 reach was increased to 310 percent. Both BC and BG Zone 3 elements see the fault. The simulation was run 12 times. Two times out of 12, the relay incorrectly determined the fault to be BG and enabled a Zone 1 BG element overreach. Ten times out of 12, the relay restrained; for these, the relay determined the fault to be BC and enabled the BC distance elements, which correctly identified the fault location to be just beyond the Zone 3 reach. The results of this test are shown in Fig. 18.

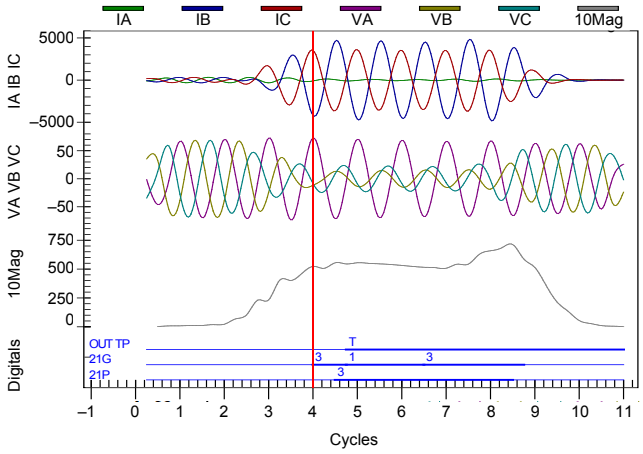

Fig. 18. Replay With Zone 1 Set to 75 Percent, Zone 3 at 310 Percent—Trip

Recall from Fig. 7 that there exists a small region of R_F at around 1 ohm where, even at a Zone 3 reach setting of 310 percent, the relay would incorrectly determine a BG fault type. Using the event data from Relays U and Z and the actual system source impedances at the time of the fault, R_F and fault location were determined.

This was accomplished by using the negative-sequence network diagram for the fault and event data recorded from relays at each end of the faulted line. The negative-sequence voltage drop equation is written from each source to the point of the fault. The negative-sequence voltage at the fault is equal, so these equations are set equal to each other to eliminate the fault voltage term. We solve for the fault location, *m*. Once the fault location is known, we can solve for the negative-sequence voltage at the fault and subsequently solve for R_F.

One observation from this exercise is that the source impedances during the fault, as recorded by event data, were different from those used in fault studies and system modeling by the utility. *Interestingly, the calculated R_F from event data during the fault was 0.92 ohms. We can now look at* Fig. 7 *and know that had the utility set the Zone 3 reach twice as large (310 percent) as the actual setting, this particular system and fault R_F would have challenged the fault-selection algorithm of the 1980s relay. The R_F value and system impedances provided "the perfect storm."*

In the third test, Zone 1 was set to 75 percent, and the Zone 3 reach was increased further to 620 percent. At this reach, the relay now securely determined the fault type as BC for every simulation. This enabled the BC distance elements, which correctly identified the fault location to be just beyond the Zone 3 reach. The results of this test are shown in Fig. 19.

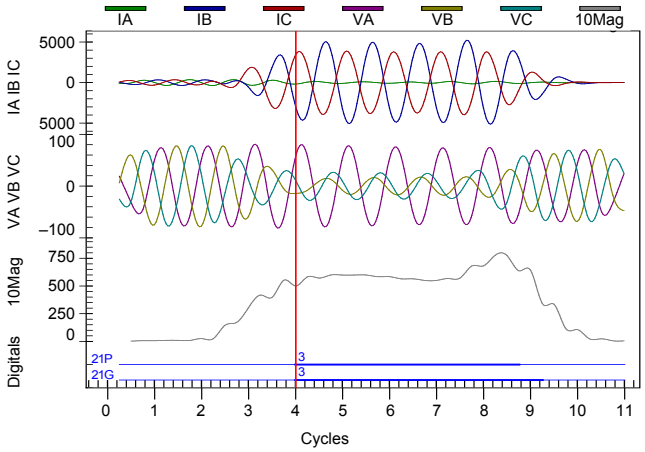

Fig. 19. Replay With Zone 1 at 75 Percent and Zone 3 at 620 Percent—No Trip

In the fourth test, the Zone 3 element reach was restored to its original 155 percent value. Because this was a short-line application, a common necessity for securing the Zone 1 elements against overreach is reducing Zone 1 reach. Fig. 20 shows that by further reducing the Zone 1 reach to 53 percent of the line, the overreach is prevented for this particular fault.

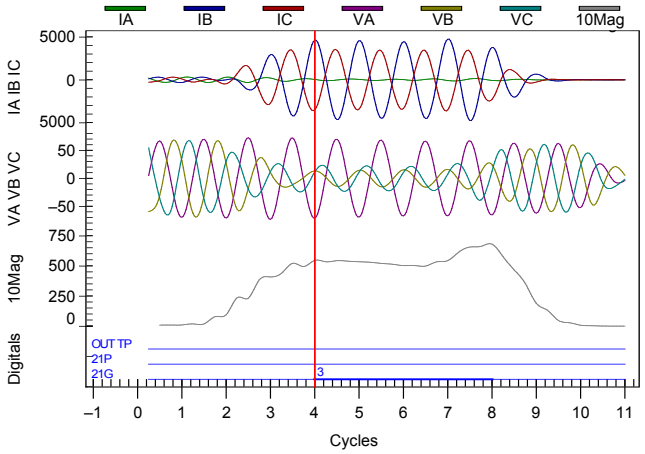

Fig. 20. Zone 1 at 53 Percent, Zone 3 at 155 Percent—No Trip

Replaying actual event data through a so-called exemplar relay in the lab is an excellent method of validating field performance and performance with different settings. It allowed us to confirm some conclusions made through Mathcad analysis—that Zone 1 reach reduction and/or Zone 3 reach extension are the two easiest means to prevent overreach for this particular fault.

E. Mathcad Simulation of State-of-the-Art Microprocessor Relay

To prove that the 1993 (and today's) relay would have been secure, its response to the event report data recorded by Relay Z during the 1999 BCG fault was simulated using Mathcad. This testing confirms the reliable performance of the improved FIDS logic. It also proves that the newer relay is not dependent on user settings for fault type selection security.

The modern relay is set with the original Zone 1 reach at 75 percent and Zone 3 reach at 155 percent of the protected line impedance. Directional element thresholds are set based on the positive-sequence line impedance.

In Fig. 21, the Mathcad worksheet plots the 49-degree angle by which IA2 lags IA0. Given this, the relay selects the phase-to-phase mho element with the lowest calculated reach (BC in this case).

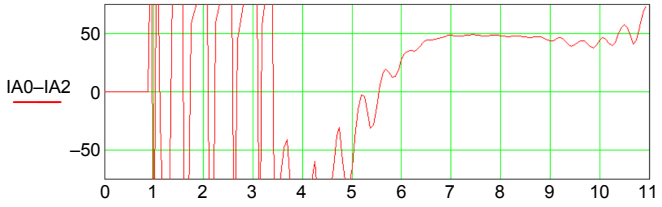

Fig. 21. IA2 Lags IA0 by 49 Degrees (Matches Original Event Data)

The relay then compares |Rag| with the R_F of |Rbc|. If |Rag| is lower, the fault involves A-phase. If not, the relay selects the phase-to-phase element (BC). This decision process is shown in Fig. 22 by the outcome of the asserted FSA60.

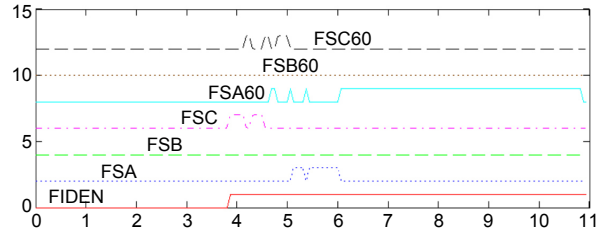

Fig. 22. Simulated FIDS Response of 1993-Era Relay to Event Data

In Fig. 23, we can see that the 1993-era, Zone 1 MBG element sees the fault within its reach. This plot shows the response of the reach calculation only and includes none of the supervision logic. In fact, even though this element sees the fault, it is blocked from operation by the modern FIDS logic, unlike the 1980s-era relay.

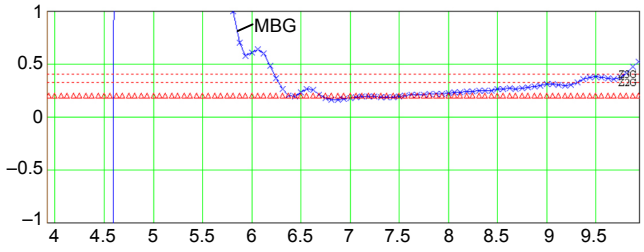

Fig. 23. MBG Distance Element Response in Mathcad Simulation of Event Data (This Element Is Blocked by FIDS Logic for This Fault)

Fig. 24 shows the logic that supervises the MBG element [10]. In order to allow operation of the Zone 1 MBG element, the relay has to enable the FSB element. For this fault, FSB remains deasserted due to improved FIDS logic. This ensures that the Zone 1 MBG element restrains and is secure during the BCG fault.

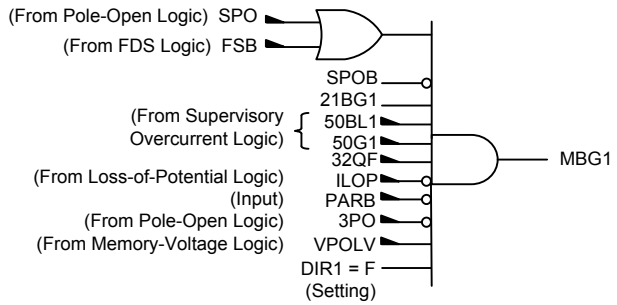

Fig. 24. Zone 1 Mho Ground Distance Element Logic

Because the relay now enables the MBC elements, these are allowed to operate if the fault is seen within their reach. Fig. 25 shows the Zone 1, 2, and 3 MBC element response to the fault data. The fault location is determined accurately by the phase-to-phase elements—just beyond the Zone 3 reach. The modern relay would not have operated for this fault. Fig. 26 shows the logic that supervises the MBC element.

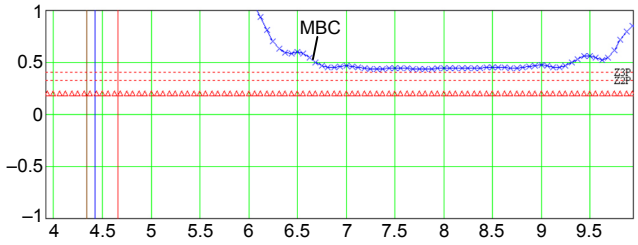

Fig. 25. MBC*x* (Where *x* Is Zone 1, 2, 3) Distance Element Response to Event Replay. No Operation. MBC*x* Would Be Allowed to Operate Per FIDs, but Fault Is Just Beyond MBC3

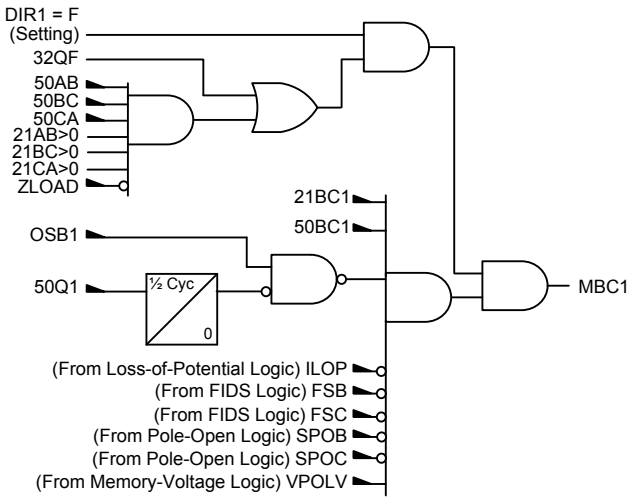

Fig. 26. Zone 1 Mho Phase Distance Element Logic

F. Replay of Original Fault Data Using COMTRADE Into State-of-the-Art Microprocessor Relay

To further validate our Mathcad model and theory, the event report data recorded by Relay Z during the 1999 BCG fault were converted to COMTRADE files and replayed into a relay in the lab. The relay was a 1993-era microprocessor relay, as described earlier.

The modern relay is set with the original Zone 1 reach at 75 percent and Zone 3 reach at 155 percent of the protected line impedance. Fig. 27 shows the relay response to the replayed fault data. As the Mathcad simulations predicted, the relay's improved FIDS logic identifies this first as either an AG or BC fault (FSA asserted). The fact that the Z1G element is shown deasserted, despite the fault being within its reach, proves that the FIDS logic definitely determined that this was a BC fault. Further, the data show that the relay determined the fault direction as forward (32QF) and did not operate by any element.

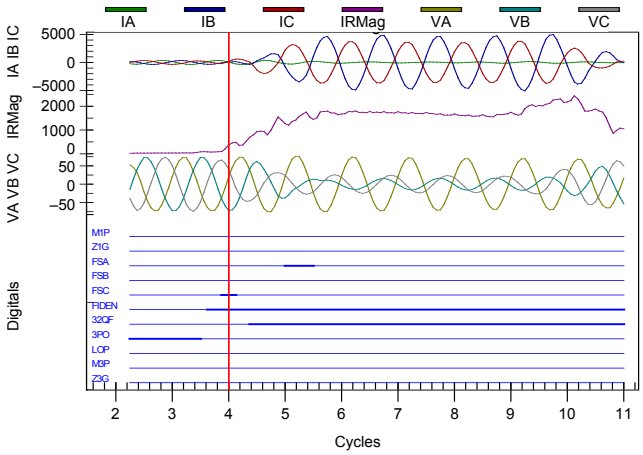

Fig. 27. Replay of Relay Z Event Data Through 1993-Era Distance Relays With Improved FIDS Logic

In summary, the modern relay, with identical settings as in the 1980s-era relay, would be secure. Detailed fault studies are not required with this relay design. Zone 3 settings can be set based on a reach required to coordinate for remote backup functions, independent of fault type selection. For the system in Case Study Number 1, the local utility elected to change settings in the 1980s relays immediately. A longer-term project to replace the 1980s relays with the modern relay was also initiated.

VI. Finding Root Cause—Case Study Number 2

A. Analysis of the Fault

In December 2007, a CAG fault with R_F occurred on a transmission line. This is Case Study Number 2. Refer to Fig. 28 for the one-line diagram.

From the event data and an ASPEN OneLiner model, the SIR is calculated to be 2.8 for Relay Victor. The line length is nearly 35 miles. Neither of these factors would be commensurate with a "short line."

The fault was located in the line section but just at or beyond the Zone 1 reach. The relays at each end of the line tripped to clear the fault, so the utility determined this operation to be "correct."

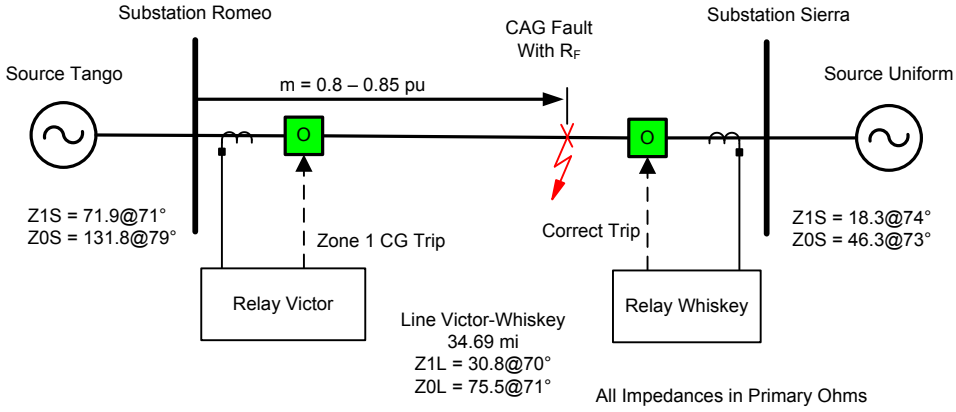

Fig. 28. Case Study Number 2 One-Line Diagram

However, upon further inspection, it can be seen that Relay Victor determined the fault type to be Zone 1 CG and possibly overreached. The event data in Fig. 29 clearly show the fault to be a CAG fault. While it is desirable to trip high speed for an in-section fault, from a manufacturer's perspective, this event would be classified as an incorrect operation due to incorrect fault type selection and possible overreach. The relay involved in Case Study Number 2 is the same model as those in Case Study Number 1.

For this paper, no event data were available from the remote line terminal.

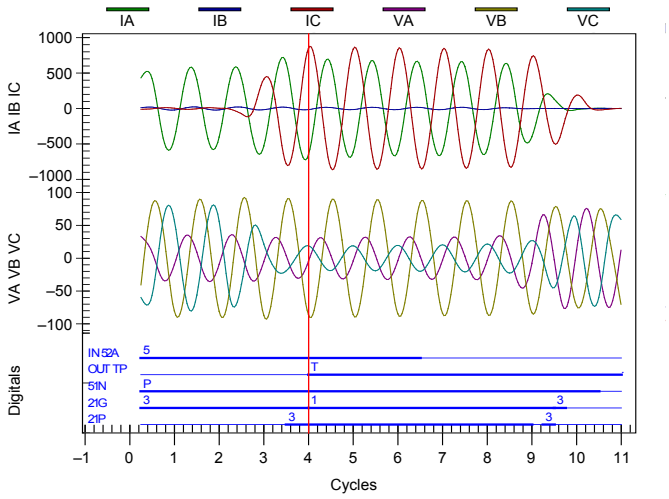

Fig. 29. Event Data From 1980s Relay Show CAG Fault and Possible Zone 1 CG Overreach

The system in Fig. 28 was modeled. A CAG fault was placed at 85 percent of the line from Substation Romeo. Torque products of the CA and CG Zone 3 elements in Relay Victor were calculated for several values of R_F and Zone 3 reach using the Mathcad worksheet shown in the appendix [6]. Fault impedance was varied from 0 to 5 ohms. Several values of Zone 3 reach were evaluated: 150 percent, 180 percent, 300 percent, and 600 percent of the protected Line Victor-Whiskey impedance. The results of the exercise are shown in Fig. 30.

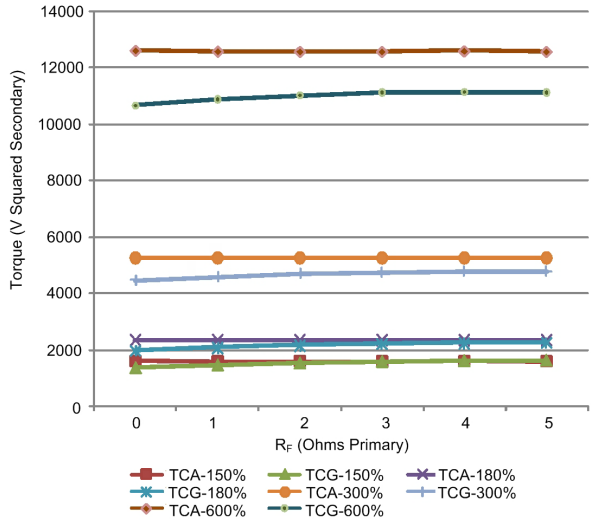

Fig. 30. CA and CG Torque Values for Different R_F and Zone 3 Reach

Several interesting conclusions can be made from Fig. 30. At increasing values of R_F, especially greater than 3 ohms, Zone 3 reach settings of 150 and 180 percent are not secure. Increasing the Zone 3 reach setting to 300 percent allows for correct CA fault identification for all values of R_F up to 5 ohms. Further increasing the Zone 3 reach setting to 600 percent allows for correct CA fault identification for all values of R_F up to 5 ohms, while allowing more margin.

Data from Relay Whiskey were not available; therefore, the actual value of R_F during the fault is not known. Regardless, the conclusion from Fig. 30 is that larger Zone 3 reach settings provide more reliable fault selection when using torque comparison.

B. Considerations for Improved Settings in the 1980s Design

Using the Mathcad worksheet in the appendix, we wanted to show some immediate steps that could be taken by the utility to prevent this and other occurrences. See Fig. 31.

With Zone 3 equal to 150 percent and an obvious CAG fault from the event waveforms, the relay declared a CG fault type and allowed the CG distance elements to run. This permitted the relay to trip by the CG Zone 1 element. Therefore, the immediate solution for this case involves running short-circuit studies, using the Mathcad tool or relay testing, and determining an increased, more secure Zone 3 reach setting. In this application, Zone 3 is enabled to trip for remote breaker failure and substation battery failure. Therefore, with an increased reach, the Zone 3 time delay must be evaluated for coordination.

1980s Relay Mho Distance Calculations:

$Re(yag) = 352.308$ $Re(ybg) = -5.544 \cdot 103$ $Re(ycg) = 1.974 \cdot 103$

$Re(yab) = -2.582 \cdot 103$ $Re(ybc) = -4.973 \cdot 103$ $Re(yca) = 1.983 \cdot 103$

$r \equiv 1.8$

$$yag := \left[r \cdot Z1Lsec \cdot ang \cdot \left(\frac{Ia}{CTR} + k \cdot \frac{Ir}{CTR}\right) - \frac{Va}{PTR}\right] \cdot \overline{VAP}$$

$$ybg := \left[r \cdot Z1Lsec \cdot ang \cdot \left(\frac{Ib}{CTR} + k \cdot \frac{Ir}{CTR}\right) - \frac{Vb}{PTR}\right] \cdot \overline{(VAP \cdot a^2)}$$

$$ycg := \left[r \cdot Z1Lsec \cdot ang \cdot \left(\frac{Ic}{CTR} + k \cdot \frac{Ir}{CTR}\right) - \frac{Vc}{PTR}\right] \cdot \overline{(VAP \cdot a)}$$

$$yab := \left[r \cdot Z1Lsec \cdot ang \cdot \left(\frac{Iab}{CTR}\right) - \left(\frac{Vab}{PTR}\right)\right] \cdot \overline{(-VAP \cdot a \cdot j)}$$

$$ybc := \left[r \cdot Z1Lsec \cdot ang \cdot \left(\frac{Ibc}{CTR}\right) - \left(\frac{Vbc}{PTR}\right)\right] \cdot \overline{(-VAP \cdot j)}$$

$$yca := \left[r \cdot Z1Lsec \cdot ang \cdot \left(\frac{Ica}{CTR}\right) - \left(\frac{Vca}{PTR}\right)\right] \cdot \overline{(-VAP \cdot a^2 \cdot j)}$$

Fig. 31. Short-Term Settings Solutions Where *r* Is the Reach Setting

C. Mathcad Simulation of State-of-the-Art Microprocessor Relay

In Fig. 32, event data show IA2 lagging IA0 by 145 degrees. As shown in Fig. 11, the relay selects BG or CA based on which element has the lowest calculated reach. The event data were replayed through a Mathcad simulation of the modern relay, and the results are shown in Fig. 33. During the first 3 cycles, the FIDS logic determines correctly that the fault type is AG. At Cycles 3 through 4, the FIDS logic determines correctly that the fault type has evolved. It asserts the FSB Relay Word bit, correctly enabling the BG and CA distance elements.

VII. Finding Root Cause—Case Study Number 3

A. Analysis of the Fault

In March 2009, an ABG fault with R_F occurred on a 138 kV transmission line. This is Case Study Number 3. Refer to Fig. 34 for the one-line diagram. The relays closest to the fault correctly tripped.

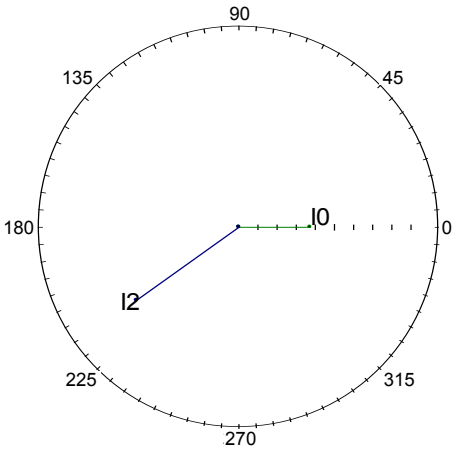

Fig. 32. IA2 Lags IA0 by 145 Degrees (at Cycle 7)

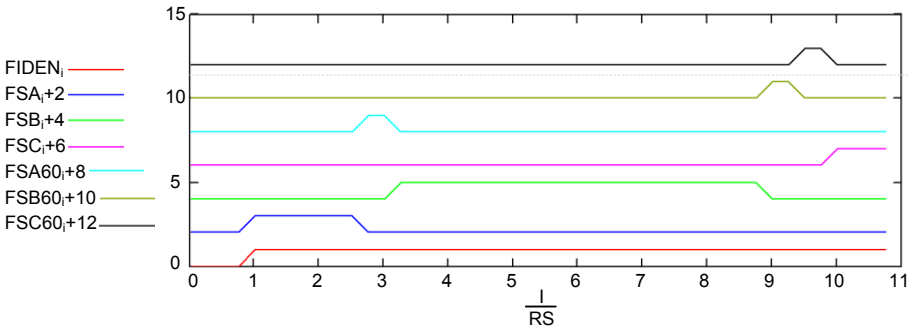

Fig. 33. Simulated FIDS Response of 1993-Era Relay to Event Data

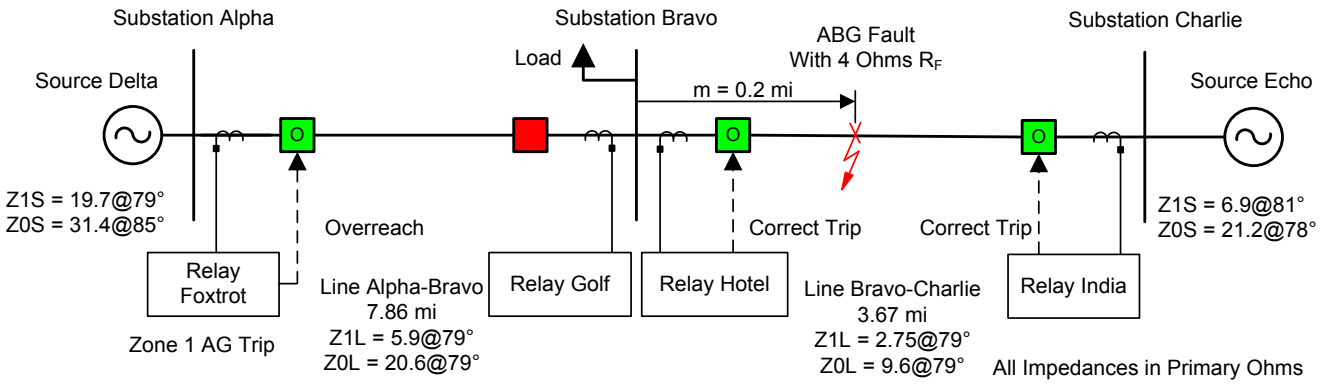

Fig. 34. Case Study Number 3 One-Line Diagram

One line section away, Relay Foxtrot incorrectly identified the fault type to be a Zone 1 AG and overreached. See Fig. 35. This caused a momentary outage of a distribution substation until automatic reclosing restored service.

Relay Foxtrot is not the same model as those in Case Study Number 1; however, they share fault type selection and distance element algorithm design. Foxtrot is the backup relay at the terminal looking to Substation Bravo. The primary relay is of the modern 1993-era design.

Using event data from Relays Foxtrot and India and the actual system source impedances at the time of the fault, R_F and fault location were determined. The SIR is calculated to be 5.2 for Relay Foxtrot. The line length is nearly 8 miles. The R_F during the fault is 4 ohms.

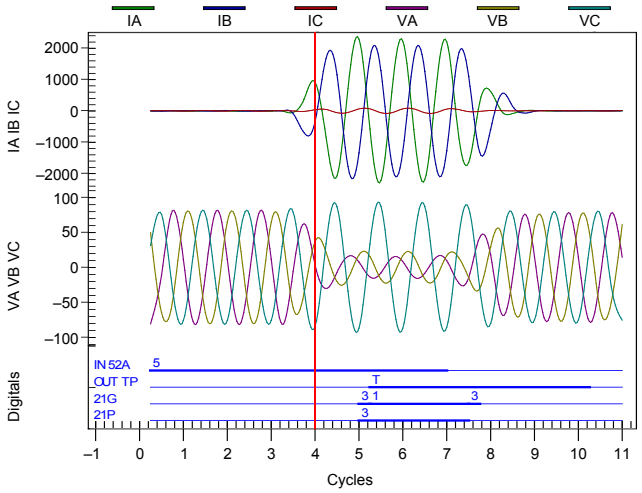

Fig. 35. Event Data From Relay Foxtrot Show ABG Fault and Zone 1 AG Overreach

B. *Considerations for Improved Settings in the 1980s Design*

Using the Mathcad worksheet in the appendix, we wanted to show some immediate steps that could be taken by the utility to prevent this and other occurrences. See Fig. 36.

Re(yag) = 891.595	Re(ybg) = 164.56	Re(ycg) = –6.064
Re(yab) = 659.906	Re(ybc) = $-4.835 \cdot 10^3$	Re(yca) = –4.498
r≡ 1.7		
Re(yag) = $2.61 \cdot 10^3$	Re(ybg) = $1.628 \cdot 10^3$	Re(ycg) = –6.824
Re(yab) = $3.039 \cdot 10^3$	Re(ybc) = $-3.948 \cdot 10^3$	Re(yca) = $-3.57 \cdot 10^3$
r≡ 3.4		

Fig. 36. Short-Term Settings Solutions Where *r* Is the Reach Setting

With Zone 3 equal to 170 percent and an obvious ABG fault from the event waveforms, the relay declared an AG fault type and allowed the AG distance elements to run. This permitted the relay to trip by the AG Zone 1 element.

The system in Fig. 34 was modeled. An ABG fault was placed at 5 percent of the line from Substation Bravo. Torque products of the AB and AG Zone 3 elements in Relay Foxtrot were calculated for several values of R_F and Zone 3 reach using the Mathcad worksheet shown in the appendix [6]. Fault impedance was varied from 0 to 10 ohms. Several values of Zone 3 reach were evaluated: 170 percent, 340 percent, and 680 percent of the protected Line Alpha-Bravo impedance. The results of the exercise are shown in Fig. 37.

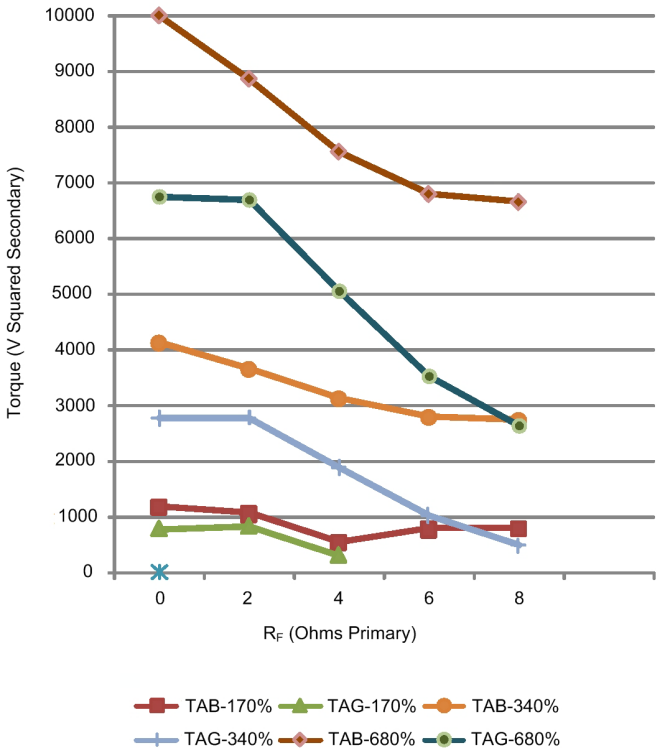

Fig. 37. AB and AG Torque Values for Different R_F and Zone 3 Reach

Several interesting conclusions can be made from Fig. 37. At R_F values near 4 ohms, a Zone 3 reach setting of 170 percent is not secure. Increasing the Zone 3 reach setting to 340 percent allows for correct AB fault identification for all values of R_F up to 10 ohms. Further increasing the Zone 3 reach setting to 680 percent allows for correct AB fault identification for all values of R_F up to 10 ohms, while allowing more margin. Recall that the actual value of R_F during the fault was determined from event data to be around 4 ohms. Again, the conclusion from Fig. 37 is that larger Zone 3 reach settings provide more reliable fault selection when using torque comparison.

The immediate solution for this case might have involved running short-circuit studies, using the Mathcad tool or relay testing, and determining an increased, more secure Zone 3 reach setting. In this application, Zone 3 was originally enabled to trip for remote breaker failure and substation battery failure. The remote substation experienced local breaker failure. However, the primary relay in this case is of the modern design and also had an identical Zone 3 backup function enabled.

The Zone 3 element within Relay Foxtrot was determined to be a "backup to a backup to a backup" and something that could be removed from service without loss of much practical benefit. The decision was then made to remove the Zone 3 element from tripping duty in the backup relay, while at the same time increasing its reach to the maximum allowed. The maximum allowed is 3,200 percent of the protected line

impedance or 64 ohms secondary, whichever is less. Thus, the Zone 3 element in Relay Foxtrot is used only for fault type selection and is as secure as possible.

C. Response of State-of-the-Art Microprocessor Relay

In Fig. 38, event data show IA2 leading IA0 by 111 degrees. As shown in Fig. 11, the relay selects CG or AB based on which element has the lowest calculated reach.

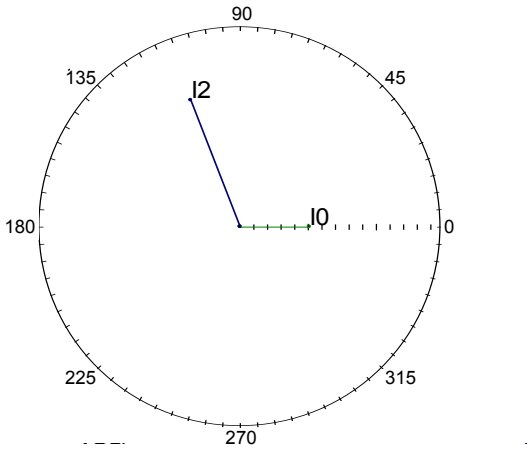

Fig. 38. IA2 Leads IA0 by 111 Degrees (at Cycle 6)

Event data from the primary relay with modern FIDS logic are shown in Fig. 39. The FIDS logic determines correctly that the fault type is CG or AB. It asserts the FSC Relay Word bit, correctly enabling the CG and AB distance elements.

From the event data in Fig. 39, we can see the ZAB distance element is enabled and active, asserting a Zone 4 and then a Zone 2 element. This is a correct operation, as the fault was just beyond the remote bus between Substations Bravo and Charlie.

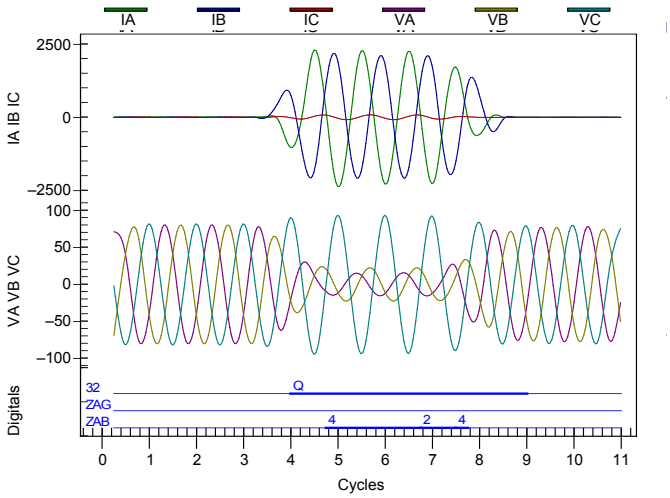

Fig. 39. Actual Relay Response of 1993-Era Relay (Primary) to Event Data

VIII. Conclusions

Consider automobile safety technology and this analogy. No one wants to be involved in an automobile crash, but if you were unfortunate enough to be involved in one, would you be safer in a 1968 or 2010 model Chevrolet Camaro?

Let us say you drive a beautifully maintained 1968 Chevrolet Camaro. A classic car fan would refer to this as "a sweet ride." For safety, it has a lap seat belt. It weighs about 3,800 pounds. However, this vehicle includes no shoulder restraint belt, no advanced frame crumple zones, no front or side curtain air bags, etc.

Fig. 40. 1968 Chevrolet Camaro

What if we purchase a new 2010 Camaro instead? This car has three-point safety belts and weighs about 3,800 pounds. More importantly, it includes electronic stability control to adjust engine torque and individual wheel brake pressure. A traction control system senses and reduces wheel spin. It includes six front- and head-curtain side-impact air bags, four-wheel antilock disc brakes, and one-piece, seamless side body panels for extra rigidity. Further, in case of a crash, automatic emergency response can be dispatched through onboard GPS (global positioning system) navigation and cell phone systems.

By 1968 standards, the Camaro was considered safe and met or exceeded all applicable standards. By today's standards, if safety were our sole concern, we would choose the 2010 model for its obvious improvements.

Fig. 41. 2010 Chevrolet Camaro

There is a state-of-the-art in any industry. Relays designed in the 1980s had 1980s technology, with its benefits and weaknesses in design. Advancements continue every day, as the 1993-era relay improvements prove.

Determining relay settings has always been considered an art and science. It is likely that the importance of the Zone 3 reach setting in fault type selection and security was not completely understood. Given the short-line applications, especially in Case Study Number 1, and with the relay and communications options available at the time, the Zone 1 and Zone 3 settings are understandable. And, determining secure settings for a given fault is always a much easier task to perform after the fault, given the benefit of hindsight and data.

Obviously, each utility had from 1993 to 1999, 2007, and 2009, respectively, to become aware of the new technology that was documented in widely publicized technical literature. Had settings changes alone not been a valid option, each had years to replace and upgrade the relays to better and more secure products. Why didn't they? It is possible that they were not aware of all the issues involved, but it was just as likely economics. After all, there are thousands of traditional relays still in service today, despite their known weaknesses in performance and reliability. Nevertheless, it does show the responsibilities of the manufacturer to communicate new technology and of the user to stay current with technology.

These cases can be considered a lesson learned for *all* engineers. Do not be the engineer who has "one year of experience ten times." Stay current on the development of new technology. Work hard to always learn, re-evaluate how you do things, and review relay applications and settings. Our shared goal is to make electric power safer, more reliable, and more economical over time.

Through root-cause investigation, the following conclusions were made:

- Three case studies were evaluated that involved the overreach of Zone 1 ground distance elements in a 1980s-era relay.
- Engineers from the utilities and manufacturer cooperatively worked to find root cause. Event analysis showed that root cause was the fault-selection logic and was related to Zone 3 reach settings in a 1980s vintage microprocessor distance relay.
- The success of the 1980s relay fault type identification is dependent on Zone 3 reach, power system operating parameters, fault location and type, and R_F during the fault.
- Of these factors, the engineer generally has control over the Zone 3 reach. In general, in the 1980s relay, a greater Zone 3 distance element reach produces more reliable faulted phase identification. If Zone 3 is not enabled as a tripping element, the simplest solution is to set the Zone 3 reach to its maximum allowed value.
- However, large Zone 3 reach settings, even if not enabled to trip, must be evaluated to ensure that they are not continuously picked up due to load.
- Setting changes can be made immediately to existing 1980s relays to improve security and reduce the risk of future occurrences. An engineer should model the power system, perform fault studies, and examine fault type selection based on Zone 3 torques to ensure that the applied settings are secure [6].
- Zone 3 elements, when enabled to trip, must be evaluated for fault type selection performance, coordination for faults, and compliance with applicable NERC (North American Electric Reliability Corporation) load limits.
- Superior FIDS logic using the relationship between negative- and zero-sequence current was developed in a newer 1993 design that is still state-of-the-art today. This logic is available in a different relay design and can provide the best solution without the need for reach settings changes. In some cases, the best course of action is to upgrade older relay installations to the state-of-the-art design.
- Engineers should work hard to stay current with state-of-the-art developments.

IX. Appendix

Case Study Number 1—Fault Near A, Relay Z Response
Distance Element Calculation Sheet

$a \equiv -0.5 + i \cdot 0.866$ $\quad rad \equiv 1$ $\quad deg \equiv \pi/180 \cdot rad$ $\quad I \equiv 1 .. 43$

Line parameters from relay settings:

$PTR \equiv 1200$ $\quad CTR \equiv 240$ $\quad MTA := 82\ deg$ $\quad LL := 2.06$

$Z1L := 1.32 \cdot e^{j \cdot 75.0 \cdot deg}$ $\quad Z0L := 4.34 \cdot e^{j \cdot 71.6 \cdot deg}$

$\arg(Z1L) = 75\ deg$ $\quad Z1Lsec := Z1L \cdot CTR/PTR$ $\quad Z0Lsec := Z0L \cdot CTR/PTR$

Prefault primary voltages for polarizing memory—obtain from prefault data in event report or system model:

$Vap1 := 81.6/.001 \cdot e^{(j \cdot 0 \cdot deg)}$ $\quad Vbp1 := 81.6/.001 \cdot e^{(j \cdot 240 \cdot deg)}$ $\quad Vcp1 := 81.6/.001 \cdot e^{(j \cdot 120 \cdot deg)}$

$Vap := Vap1$ $\quad Vbp := Vbp1$ $\quad Vcp := Vcp1$

Enter the primary fault quantities from event report or system model:

$Va := 89.5/.001 \cdot e^{(j \cdot 1.0 \cdot deg)}$ $\quad Ia := 637 \cdot e^{(j \cdot -62 \cdot deg)}$

$Vb := 16.5/.001 \cdot e^{j \cdot 176 \cdot deg}$ $\quad Ib := 6348 \cdot e^{j \cdot 176 \cdot deg}$

$Vc := 26.9/.001 \cdot e^{(j \cdot 119.0 \cdot deg)}$ $\quad Ic := 4970 \cdot e^{(j \cdot 19 \cdot deg)}$

$Ir := Ia + Ib + Ic$

Symmetrical components (for ABC system rotation):

$Va0 := 1/3 \cdot (Va + Vb + Vc)$	$\lvert Va0\rvert = 2.182 \cdot 10^4$	zero-sequence volts primary
$Va2 := 1/3 \cdot (Va + a^2 \cdot Vb + a \cdot Vc)$	$\lvert Va2\rvert = 2.841 \cdot 10^4$	negative-sequence volts
$Va1 := 1/3 \cdot (Va + a \cdot Vb + a^2 \cdot Vc)$	$\lvert Va1\rvert = 4.146 \cdot 10^4$	positive-sequence volts
$Ia0 := 1/3 \cdot (Ia + Ib + Ic)$	$\lvert Ia0\rvert = 668.796$	zero-sequence amperes primary
$Ia1 := 1/3 \cdot (Ia + a \cdot Ib + a^2 \cdot Ic)$	$\lvert Ia1\rvert = 3.783 \cdot 10^3$	positive-sequence amperes
$Ia2 := 1/3 \cdot (Ia + a^2 \cdot Ib + a \cdot Ic)$	$\lvert Ia2\rvert = 2.654 \cdot 10^3$	negative-sequence amperes

$\arg(Va0) = 23.627\ deg$ $\quad \arg(Ia0) = 131.683\ deg$

$\arg(Va1) = -6.341\ deg$ $\quad \arg(Ia1) = -79.163\ deg$

$\arg(Va2) = -5.263\ deg$ $\quad \arg(Ia2) = 89.297\ deg$

$k := (Z0L - Z1L)/3 \cdot Z1L$ $\quad |k| = 0.763$ $\quad \arg(k) = -4.884\ deg$

$VAP := 1/3 \cdot (Vap/PTR + a \cdot Vbp/PTR + a^2 \cdot Vcp/PTR)$

$|VAP| = 67.999$ $\quad \arg(VAP) = 7.278 \times 10^{-4}\ deg$

$VABm := VAP - a^2 \cdot VAP$ $\quad VBCm := a^2 \cdot VAP - (a \cdot VAP)$ $\quad VCAm := a \cdot VAP - VAP$

LNANG := arg(Z1L)

SHIFT := MTA − LNANG

ang := exp(j • SHIFT • deg) SHIFT = 7 deg

Vab := Va − Vb Vbc := Vb − Vc Vca := Vc − Va

Iab := Ia − Ib Ibc := Ib − Ic Ica := Ic − Ia

$Tag := [r \cdot Z1Lsec \cdot ang \cdot (Ia/CTR + k \cdot Ir/CTR) - Va/PTR] \cdot \overline{VAP}$

$Tbg := [r \cdot Z1Lsec \cdot ang \cdot (Ib/CTR + k \cdot Ir/CTR) - Vb/PTR] \cdot \overline{\left(VAP \cdot a^2\right)}$

$Tcg := [r \cdot Z1Lsec \cdot ang \cdot (Ic/CTR + k \cdot Ir/CTR) - Vc/PTR] \cdot \overline{\left(VAP \cdot a\right)}$

$Tab := [r \cdot Z1Lsec \cdot ang \cdot (Iab/CTR) - (Vab/PTR)] \cdot \overline{\left(-VAP \cdot a \cdot j\right)}$

$Tbc := [r \cdot Z1Lsec \cdot ang \cdot (Ibc/CTR) - (Vbc/PTR)] \cdot \overline{\left(-VAP \cdot j\right)}$

$Tca := [r \cdot Z1Lsec \cdot ang \cdot (Ica/CTR) - (Vca/PTR)] \cdot \overline{\left(-VAP \cdot a^2 \cdot j\right)}$

Mho distance calculations:

$Re(Tag) = -5.164 \cdot 10^3$ Re(Tbg) = 452.089 Re(Tcg) = −980.658

$Re(Tab) = -4.586 \cdot 10^3$ Re(Tbc) = 3.14 $Re(Tca) = -5.276 \cdot 10^3$

r ≡ 1.55 r = distance element reach setting in per unit of the line

Z2S := −Va2/Ia2 Z0S := −Va0/Ia0

|Z2S| = 10.704 |Z0S| = 32.633

arg(Z2S) = 85.44 deg

arg(Z0S) = 71.944 deg

If the mho element torque is positive, the fault is inside the zone. If the mho element torque is negative, the element is not asserted. Larger torque in Zone 3 determines fault type selection.

X. Acknowledgments

The authors gratefully acknowledge the work of Ed Schweitzer, Joe Mooney, and Jeff Roberts for teaching us about fault selection, distance elements, and relay operation, Normann Fischer for assistance with Mathcad simulations, and George Alexander for assistance with fault-study simulations.

Event reports shared in this paper come from actual field installations. Any reference to the original user has been removed; the relevant information comes from the event data and what lessons these data provide. The continued sharing of these event data is invaluable to our industry, greatly appreciated, and makes coming to work fun.

XI. References

[1] D. Costello and K. Zimmerman, "Distance Element Improvements – A Case Study," proceedings of the 62nd Annual Georgia Tech Protective Relaying Conference, Atlanta, GA, May 2008. Available: http://www.selinc.com.

[2] E. Price and T. Einarsson, "The Performance of Faulted Phase Selectors Used in Transmission Line Distance Applications," proceedings of the 34th Annual Western Protective Relay Conference, Spokane, WA, October 2007.

[3] SEL-121F/-221F Instruction Manual, Schweitzer Engineering Laboratories, Inc., Pullman, WA. Available: http://www.selinc.com.

[4] E. O. Schweitzer, III, "New Developments in Distance Relay Polarization and Fault Type Selection," presented at the 16th Annual Western Protective Relay Conference, Spokane, WA, October 1989. Available: http://www.selinc.com.

[5] U.S. Patent 5,140,492 titled "Distance Relay Using a Polarizing Voltage," Aug. 18, 1992. Available: http://www.uspto.gov.

[6] D. Costello and K. Zimmerman, "Effect of Zone 3 Settings on Fault Type Selection in SEL-121F, SEL-121S, SEL-121-0, SEL-221F, SEL-221S, and SEL-221-16 Relays," SEL Application Guide 2009-09, (includes SEL-121F Mathcad worksheet and SEL-121F Excel worksheet). Available: http://www.selinc.com.

[7] E. O. Schweitzer, III and J. Roberts, "Distance Relay Element Design," proceedings of the 46th Annual Conference for Protective Relay Engineers, College Station, TX, April 1993. Available: http://www.selinc.com.

[8] U.S. Patent 5,325,061 titled "Computationally-Efficient Distance Relay for Power Transmission Lines," June 28, 1994. Available: http://www.uspto.gov.

[9] U.S. Patent 5,515,227 titled "Fault Identification System for Use in Protective Relays for Power Transmission Lines," May 7, 1996. Available: http://www.uspto.gov.

[10] SEL-321 Instruction Manual, Schweitzer Engineering Laboratories, Inc., Pullman, WA. Available: http://www.selinc.com.

XII. Biographies

David Costello graduated from Texas A&M University in 1991 with a BSEE. He worked as a system protection engineer at Central Power and Light and Central and Southwest Services in Texas and Oklahoma. He has served on the System Protection Task Force for ERCOT. In 1996, David joined Schweitzer Engineering Laboratories, Inc., where he has served as a field application engineer and regional service manager. He presently holds the title of senior application engineer and works in Boerne, Texas. He is a senior member of IEEE, a member of the planning committee for the conference for Protective Relay Engineers at Texas A&M University, and a recipient of the 2008 Walter A. Elmore Best Paper Award from the Georgia Institute of Technology Protective Relaying Conference.

Karl Zimmerman is a senior power engineer with Schweitzer Engineering Laboratories, Inc. in Fairview Heights, Illinois. His work includes providing application and product support and technical training for protective relay users. He is an active member of the IEEE Power System Relaying Committee and chairman of the Task Force on Distance Element Performance with Non-Sinusoidal Inputs. Karl received his BSEE degree at the University of Illinois at Urbana-Champaign and has over 20 years of experience in the area of system protection. He is a past speaker at many technical conferences and has authored over 20 papers and application guides on protective relaying.

Previously presented at the 2010 Texas A&M Conference for Protective Relay Engineers.

20151209 • TP6386-01